

LA-3403

c.1

**DO NOT CIRCULATE**

**PERMANENT RETENTION**

**LOS ALAMOS SCIENTIFIC LABORATORY  
of the  
University of California**

LOS ALAMOS • NEW MEXICO

**Thermal Neutron Spectra  
from an Underground Nuclear Explosion  
with Special Consideration of Spectral Modification  
due to Bomb Debris Motion**

LOS ALAMOS NATIONAL LABORATORY



3 9338 00373 8514

UNITED STATES  
ATOMIC ENERGY COMMISSION  
CONTRACT W-7405-ENG. 36

## LEGAL NOTICE

This report was prepared as an account of Government sponsored work. Neither the United States, nor the Commission, nor any person acting on behalf of the Commission:

A. Makes any warranty or representation, expressed or implied, with respect to the accuracy, completeness, or usefulness of the information contained in this report, or that the use of any information, apparatus, method, or process disclosed in this report may not infringe privately owned rights; or

B. Assumes any liabilities with respect to the use of, or for damages resulting from the use of any information, apparatus, method, or process disclosed in this report.

As used in the above, "person acting on behalf of the Commission" includes any employee or contractor of the Commission, or employee of such contractor, to the extent that such employee or contractor of the Commission, or employee of such contractor prepares, disseminates, or provides access to, any information pursuant to his employment or contract with the Commission, or his employment with such contractor.

This report expresses the opinions of the author or authors and does not necessarily reflect the opinions or views of the Los Alamos Scientific Laboratory.

Printed in USA. Price \$3.00. Available from the Clearinghouse for Federal Scientific and Technical Information, National Bureau of Standards, United States Department of Commerce, Springfield, Virginia

**LOS ALAMOS SCIENTIFIC LABORATORY**  
**of the**  
**University of California**

**LOS ALAMOS • NEW MEXICO**

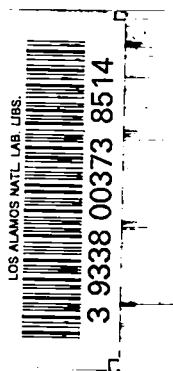
Report written: August 1965

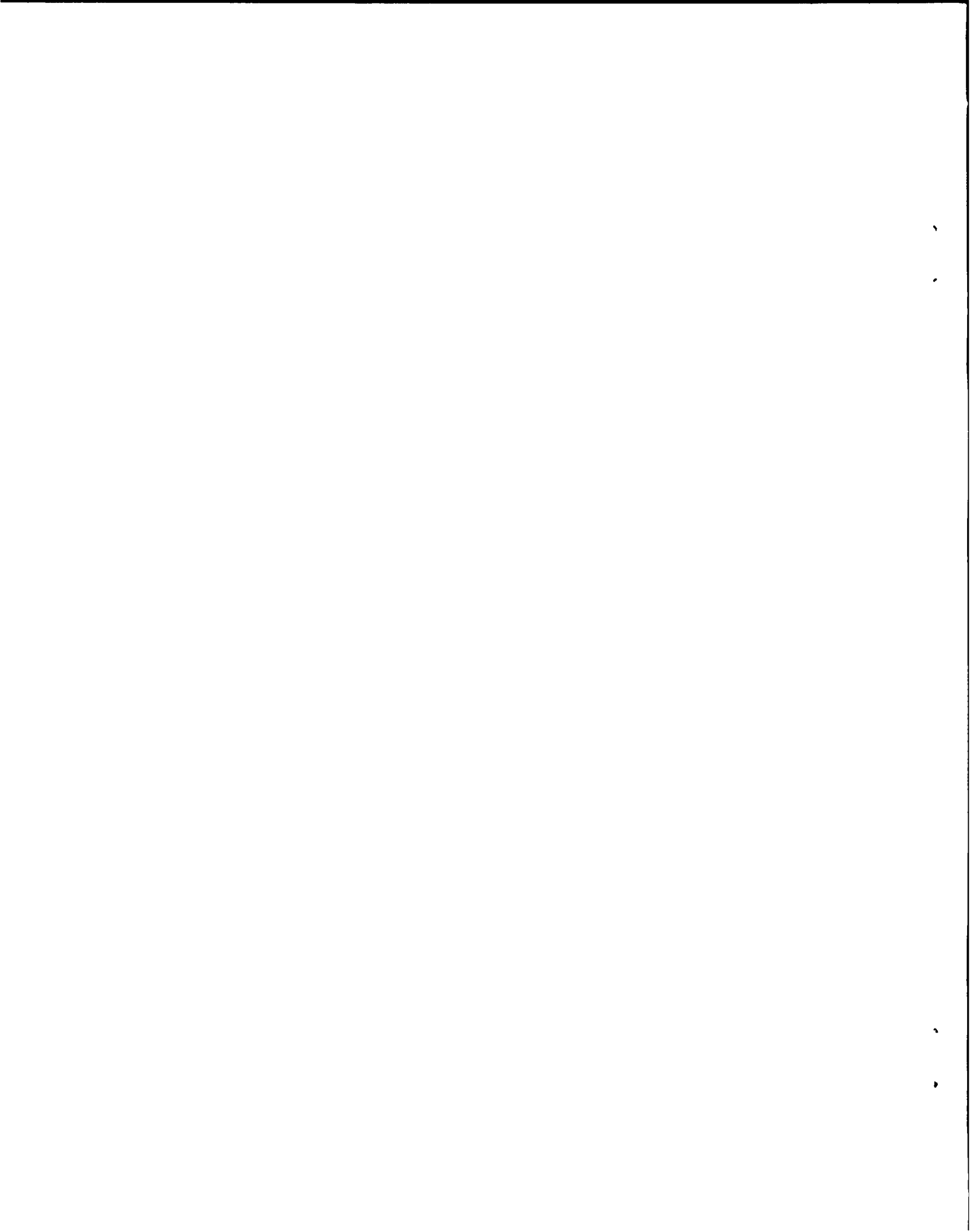
Report distributed: November 12, 1965

**Thermal Neutron Spectra**  
**from an Underground Nuclear Explosion**  
**with Special Consideration of Spectral Modification**  
**due to Bomb Debris Motion**

by

Henry A. Sandmeier and Gordon E. Hansen





## ABSTRACT

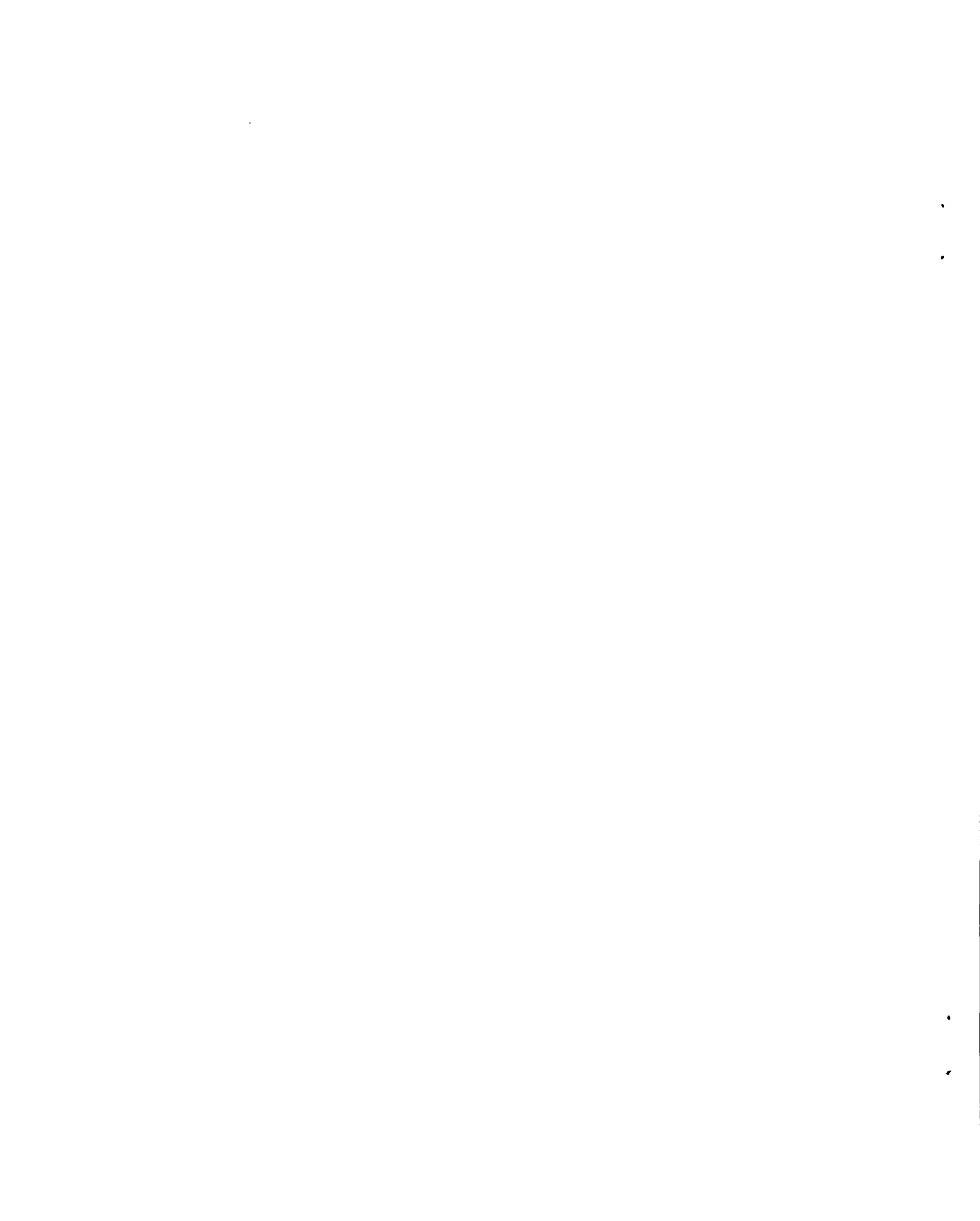
The neutron flux from an underground nuclear explosion has recently been used to measure nuclear cross sections. For the experimenter it is of interest to know the neutron spectrum and intensity emerging from the top of the pipe leading to the nuclear device.

A short time following the nuclear explosion and after many fast neutrons have escaped, the local neutron spectra in the bomb debris will be in thermal equilibria. The spectrum of neutrons leaking from this debris will depend on a superposition of these local Maxwell Boltzmann distributions each with its characteristic drift velocity  $\vec{v}_0$ .

Theoretical expressions are derived for the low energy neutron spectrum emerging from a long narrow pipe. The theoretical predictions agree reasonably well with measurements obtained from the Parrot Shot in Nevada in the Spring of 1965.

## ACKNOWLEDGMENT

We would like to thank our colleagues, Walter Goad and George Bell, for their help in this investigation.



## CONTENTS

	Page
Abstract . . . . .	3
Acknowledgment . . . . .	3
Section I. Introduction . . . . .	7
Section II. Thermal Neutron Spectra from a Rapidly Expanding Material Sphere. . . . .	10
Section III. "Pencil" Model . . . . .	16
Section IV. "Sphere" Model . . . . .	19
Section V. Numerical Evaluation of "Parrot" Escape Spectrum . . . . .	22
Section VI. Effect of Finite Bomb Debris Sphere on Measurement. . . . .	30
Appendix A. The distribution in flight time of neutrons reaching a detector remote from a pulsed source	35
Appendix B. Total source strength. . . . .	43
Appendix C. Relationship between $N(t)$ (neuts/cm <sup>2</sup> /sec) at fission foil and $n(E)$ (neuts/Mev) at point of explosion. . . . .	47

## TABLES

Table 1.	28
----------	----

CONTENTS (Continued)

		Page
ILLUSTRATIONS		
Fig. 1.	Schematic of Debris Sphere and Pipe . . . . .	8
Fig. 2.	Cylindrical Section of Debris Sphere and Pipe	12
Fig. 3.	"Pencil" Model of Debris Sphere and Pipe. . .	17
Fig. 4.	"Sphere" Model of Debris Sphere and Pipe. . .	20
Fig. 5.	Underground Nuclear Test "Parrot" . . . . .	23
Fig. 6.	Thermal Neutron Spectra. Bomb Thermal KT = 474 ev . . . . .	29
Fig. 7.	Model A and B for Neutron Source in Debris Sphere. . . . .	31
Fig. 8.	Counts at Detector for Debris Sphere Model A and B . . . . .	34
Fig. A-1.	Source--Observer Configuration . . . . .	36
Fig. A-2.	Finite Source AR and Time of Flight . . . . .	40



## I. INTRODUCTION

The problem to be solved is: given a spherical ball of bomb debris moving radially outwards with material velocity  $\vec{v}_0$  and containing neutrons in local thermal equilibria, then what is the neutron spectrum on top of a long narrow pipe of length  $R$  and radius  $\eta$  (Fig. 1). It is assumed that the debris density has become so small that no further neutron collisions will occur; in other words, the neutrons do not find a diffusive medium anymore. The neutrons are therefore liberated from a moving source containing "bottled up" neutrons with local Maxwell Boltzmann distributions. The spectrum on top of the pipe will depend on how much one "sees" of the bomb debris sphere looking down the long narrow pipe. This problem has been discussed previously by Nordheim,<sup>1</sup> as well as Bell.<sup>2</sup> This paper looks at the problem in a more general way, and the case treated by Nordheim and Bell becomes here a special case where the observer looking down the pipe sees only a "pencil" of the bomb debris sphere.

---

<sup>1</sup>L. W. Nordheim: Neutron Spectra from a Moving Source, Los Alamos Scientific Laboratory Memorandum, July 30, 1964, and Addendum, July 22, 1964.

<sup>2</sup>G. I. Bell, private communication, August 19, 1964.

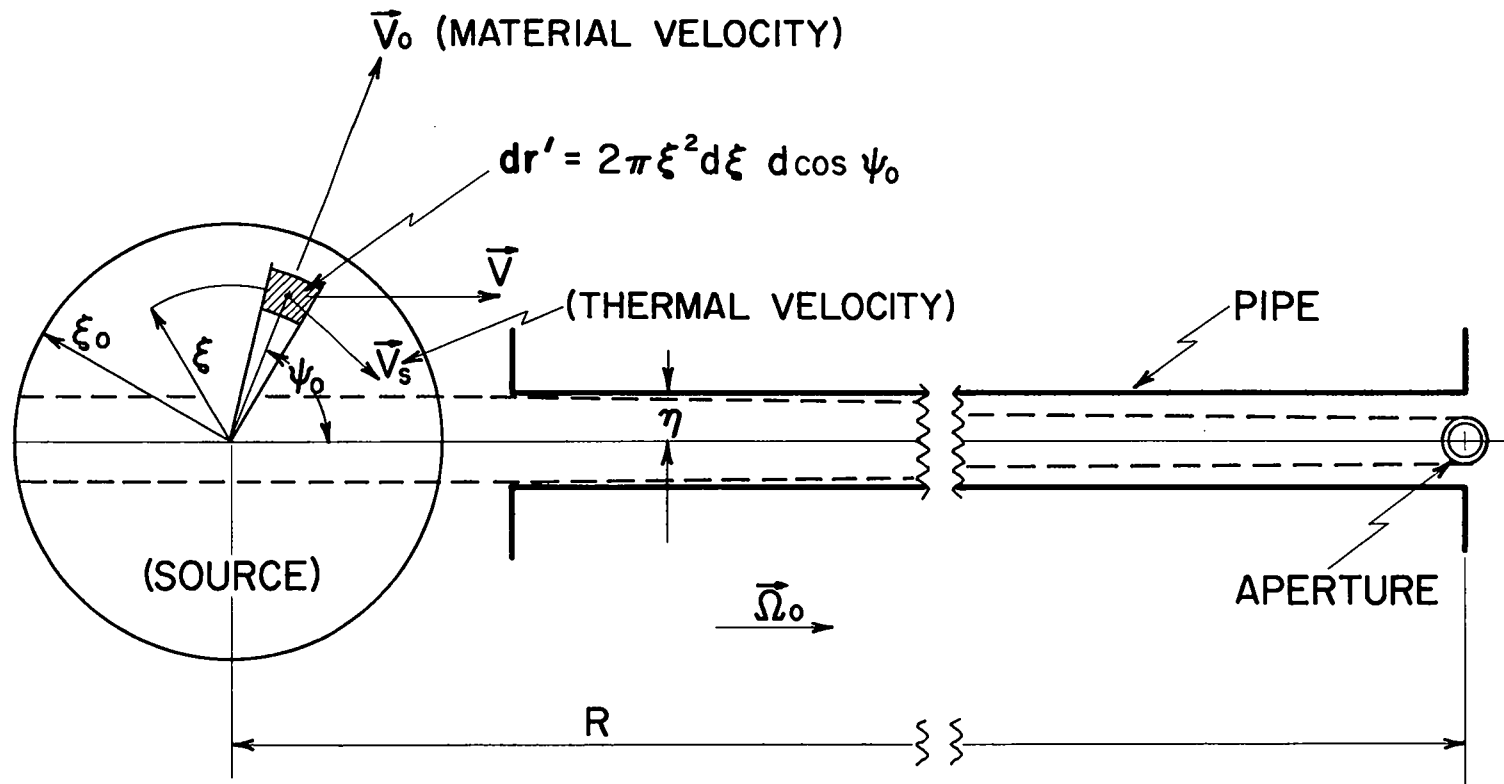


FIG. 1. SCHEMATIC OF DEBRIS SPHERE AND PIPE.

In Section II we derive the general case where the observer sees a general portion of the debris sphere.

Subsequently in Sections III and IV we discuss two special cases called the "pencil" model and the "spherical" model. As the name implies, we will see the whole sphere in the "spherical" model, and in the "pencil" model we only see a small pencil-like section of the debris sphere. In Section V we give the numerical bomb parameters relevant to this investigation. The theoretical predictions of the neutron spectrum on top of the pipe are compared with the experimental data from the "Parrot" shot.

The effect of the finite bomb debris sphere on measurements is investigated in Section VI.

## II. THERMAL NEUTRON SPECTRA FROM A RAPIDLY EXPANDING MATERIAL SPHERE

The initial neutron density in the debris is assumed to be a Maxwell-Boltzmann distribution.

$$n(\vec{v}_s) = ce^{-\frac{1}{2} m \frac{(\vec{v}-\vec{v}_0)^2}{KT}} = ce^{-\frac{1}{2} \frac{mv_s^2}{KT}} \quad \text{EQN 1}$$

Here the drift velocity is equal to the material velocity  $\vec{v}_0$ , and  $\vec{v}_s$  is the neutron velocity relative to  $\vec{v}_0$ . In Appendix A we derived an expression for the number of neutrons passing through the unit area perpendicular to direction  $\vec{\Omega}_0$  at R (Fig. 1) in the time interval  $\Delta T$  about T. The initial neutron population  $n(\vec{r}', v, \vec{\Omega}_0, 0^+)$  in Eqn. A-14 created by the  $\delta$ -function source becomes

$$n(\vec{r}', v, \vec{\Omega}_0, 0^+) = c(\vec{\xi}) e^{-\frac{1}{2} \frac{m}{KT} [v^2 + v_0^2 - 2vv_0 \cos\psi_0]} \times v^2 \quad \text{EQN 2}$$

and Eqn. A-14 becomes

$$J_0(\vec{r}, T) \Delta T = \int_{\text{source}} 2\pi \xi^2 d\xi d\cos\psi_0 c(\vec{\xi}) e^{-\frac{m}{2KT} [v^2 + v_0^2 - 2vv_0 \cos\psi_0]} \times v^2 \frac{\Delta v}{R^2} \quad \text{EQN 3}$$

CASE I: uniform gas, i.e.  $c(\xi) = \text{const.}$

from  $\xi = 0$  to  $\xi = \xi_0$ ;  $v_0 = \text{const.}$

The assumption made above means that the neutron production is uniform over the debris sphere and the debris velocity is constant in the radial direction. The evaluation of Eqn. 3 is split into three intervals (Fig. 2), i.e. regions I, II, and III. The limits of variable  $\cos\psi_0$  in the integrals are reversed because  $-d\cos\psi_0 = \sin\psi_0 d\psi_0$ . We get in the three regions

$$\begin{aligned} \frac{J_0(\vec{r}, T)\Delta T}{\Delta v} = & 2\pi \int_0^{\xi_0} \xi^2 d\xi \frac{cv^2}{R^2} \left[ \int_{\cos\psi_{00}}^{1.0} d\cos\psi_0 e^{-\frac{m}{2KT} [v^2 + v_0^2 - 2vv_0 \cos\psi_0]} + \right. \\ & \left. + \int_{-1.0}^{-\cos\psi_{00}} d\cos\psi_0 e^{-\frac{m}{2KT} [v^2 + v_0^2 - 2vv_0 \cos\psi_0]} \right] + \\ & + 2\pi \int_{-\cos\psi_{00}}^{+\cos\psi_{00}} d\cos\psi_0 \frac{cv^2}{R^2} e^{-\frac{m}{2KT} [v^2 + v_0^2 - 2vv_0 \cos\psi_0]} \int_0^{\eta/\sin\psi_0} \xi^2 d\xi \end{aligned}$$

EQN 4

In the 3rd term in Eqn. 4 we assume that

$$\int_0^{\eta/\sin\psi_0} \xi^2 d\xi = \frac{\eta^3}{\langle \sin^3\psi_0 \rangle_3}$$

EQN 5

and that the average value of  $\sin\psi_0$  or  $\langle \sin\psi_0 \rangle$  can be found graphically over region III in Fig. 2. This step is convenient to obtain a

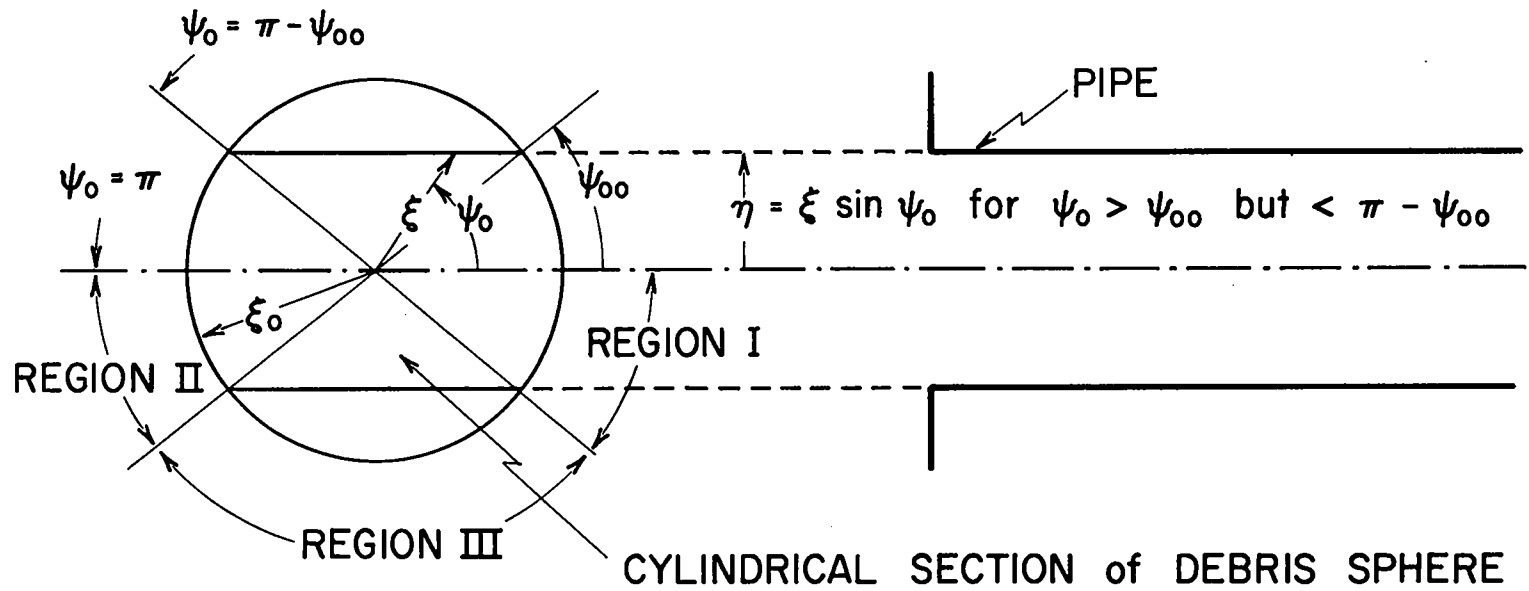


FIG. 2. CYLINDRICAL SECTION OF DEBRIS SPHERE AND PIPE.

simple solution for the 3rd term in Eqn. 4.

After solving for the definite integrals in Eqn. 4 we get

$$\begin{aligned}
 \frac{J_o(\vec{r}, T) \Delta T}{\Delta v} = & \frac{2\pi\xi_o^3 cvKT}{3m v_o R^2} \left[ e^{-\frac{m}{2KT} (v-v_o)^2} - e^{-\frac{m}{2KT} (v^2+v_o^2-2vv_o \cos\psi_{oo})} + \right. \\
 & \left. + e^{-\frac{m}{2KT} (v^2+v_o^2+2vv_o \cos\psi_{oo})} - e^{-\frac{m}{2KT} (v+v_o)^2} \right] + \\
 & + \frac{2\pi\eta^3 cvKT}{3m v_o \langle \sin^3 \psi_o \rangle R^2} \left[ e^{-\frac{m}{2KT} (v^2+v_o^2-2vv_o \cos\psi_{oo})} - \right. \\
 & \left. - e^{-\frac{m}{2KT} (v^2+v_o^2+2vv_o \cos\psi_{oo})} \right]
 \end{aligned} \tag{EQN 6}$$

or rearranging

$$\begin{aligned}
 \frac{J_o(\vec{r}, T) \Delta T}{\Delta v} = & \frac{2\pi\xi_o^3 cvKT}{3m v_o R^2} \left\{ e^{-\frac{m}{2KT} (v-v_o)^2} - e^{-\frac{m}{2KT} (v+v_o)^2} + \right. \\
 & + \left[ \frac{\eta^3}{\xi_o^3 \langle \sin^3 \psi_o \rangle} - 1 \right] \left[ e^{-\frac{m}{2KT} (v^2+v_o^2-2vv_o \cos\psi_{oo})} \right. \\
 & \left. \left. - e^{-\frac{m}{2KT} (v^2+v_o^2+2vv_o \cos\psi_{oo})} \right] \right\}
 \end{aligned} \tag{EQN 7}$$

From Appendix B, Eqn. B-10, we get for the constant c in Eqn. 7

$$c = \frac{N_o}{V_o} \left( \frac{2\pi KT}{m} \right)^{-3/2} \quad \text{EQN 8}$$

where

$N_o$  = total thermal neutrons produced in sphere

$V_o$  = sphere volume in  $\text{cm}^3$

We insert Eqn. 8 into Eqn. 7

$$\begin{aligned} \frac{J_o(\vec{r}, T) \Delta T}{\Delta v} = & \frac{N_o}{4\pi R^2} \frac{v}{v_o} \left( \frac{m}{2\pi KT} \right)^{1/2} \left\{ e^{-\frac{m}{2KT} (v-v_o)^2} - e^{-\frac{m}{2KT} (v+v_o)^2} + \right. \\ & + \left[ \frac{\eta^3}{\xi_o^3 \langle \sin^3 \psi_o \rangle} - 1 \right] \left[ e^{-\frac{m}{2KT} (v^2+v_o^2-2vv_o \cos \psi_{oo})} \right. \\ & \left. \left. - e^{-\frac{m}{2KT} (v^2+v_o^2+2vv_o \cos \psi_{oo})} \right] \right\} \quad \text{EQN 9} \end{aligned}$$

We introduce the following relationship between  $v_o$ , the material debris velocity, and the neutron temperature  $KT$

$$\frac{mv_o^2}{2KT} = \beta \quad \text{EQN 10}$$

also

$$u = \frac{v}{v_o} \quad \text{EQN 11}$$

We insert Eqns. 10 and 11 into Eqn. 9 and get finally for the general



case

$$\begin{aligned}
 J_o(\vec{r}, T) \Delta T = & \frac{N_o}{4\pi R^2} \sqrt{\frac{\beta}{\pi}} v \Delta v \left\{ e^{-\beta(v-1)^2} - e^{-\beta(v+1)^2} + \right. \\
 & + \left[ \frac{\eta^3}{\xi_o^3 \langle \sin^3 \psi_o \rangle} - 1 \right] \left[ e^{-\beta(v^2+1-2v \cos \psi_{oo})} \right. \\
 & \left. \left. - e^{-\beta(v^2+1+2v \cos \psi_{oo})} \right] \right\} \quad \text{EQN 12}
 \end{aligned}$$

Equation 12 gives the number of neutrons passing through the unit area perpendicular to  $\vec{\Omega}_o$  at  $\vec{r}$  (Fig. A-1) in the time interval  $\Delta T$  about  $T$  in terms of that portion of the initial neutron population at  $\vec{r}'$  with energies specified by  $\Delta v$  about  $v$ . This is for the general case in Fig. 2 where an observer, looking down the pipe, "sees" a general portion of the neutron generating sphere.

This general case in Eqn. 12 is not exploited numerically in this paper, but in the following we treat two practical cases which represent the two limiting cases to the general case expressed in Eqn. 12. The first case is called the "pencil" model where the observer looking down the pipe sees only a small narrow pencil-like section of the neutron producing sphere. The second case is called the "spherical" model where the observer sees the whole neutron producing sphere.

### III. "PENCIL" MODEL

Here the observer sees only a small narrow pencil-like section of the neutron producing sphere (Fig. 3). For this case it follows from Eqn. 3, Eqn. B-10, and evaluating the exponential term in Eqn. 3 for  $\cos\psi_0 \sim 1$  and  $\cos\psi_0 \sim -1$

$$J_0(\vec{r}, T)\Delta T = \frac{N_0}{V_0} \left(\frac{2\pi kT}{m}\right)^{-3/2} \frac{U_0 v^2 \Delta v}{2R^2} \left[ e^{-\frac{m}{2kT} (v-v_0)^2} + e^{-\frac{m}{2kT} (v+v_0)^2} \right]$$

EQN 13

Multiplying Eqn. 13 by  $\pi r^2$ , the aperture area of the pipe, and using the bomb parameter value  $\beta = mv_0^2/2kT = 1$  (see Section V), we have

$$\pi r^2 J_0(\vec{r}, T)\Delta t = \frac{r^2}{4R^2} \frac{N_0}{\sqrt{2\pi}} 2\sqrt{2} \frac{U_0}{V_0} v^2 \Delta v \left[ e^{-(v-1)^2} + e^{-(v+1)^2} \right]$$

EQN 14

where  $U_0$  = pencil volume in  $\text{cm}^3$ ,  $V_0$  = sphere volume in  $\text{cm}^3$ ,  $N_0$  = total thermal neutrons produced,  $v = v/v_0$ , and  $v_0 = \sqrt{2kT/m}$ . Equation 14 gives the total neutrons passing through the aperture area  $\pi r^2$  ( $\text{cm}^2$ ) on top of the pipe perpendicular to  $\vec{\Omega}_0$  at distance  $R$  (cm) from the source.

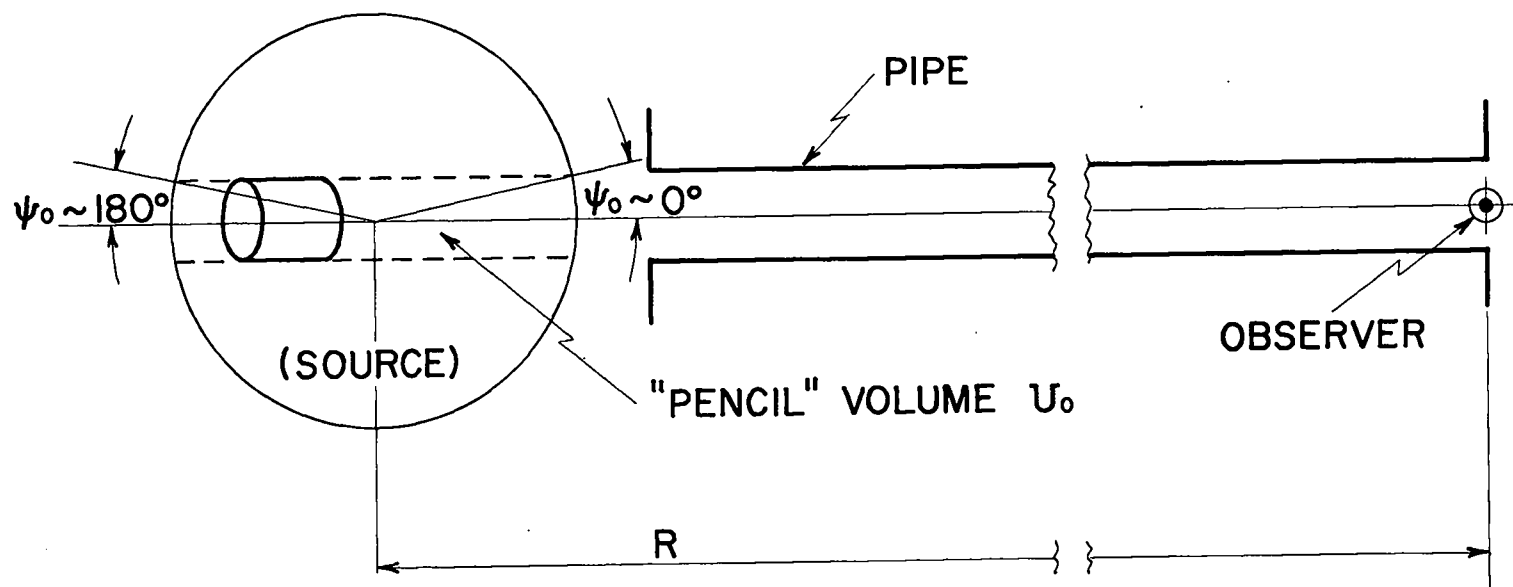


FIG. 3. "PENCIL" MODEL OF DEBRIS SPHERE AND PIPE.

For comparison, we give below the corresponding equation for the hypothetical case of  $v_0 = 0$ .

$$\pi r^2 J_0(\vec{r}, T) \Delta T = \frac{r^2}{2R^2} \frac{N_0}{\sqrt{2\pi}} \frac{1}{\sqrt{\frac{KT}{m} \frac{KT}{m}}} \frac{U_0}{V_0} v^2 \Delta v e^{-\frac{mv^2}{2KT}} \quad \text{EQN 14a}$$

#### IV. "SPHERE" MODEL

Here the observer sees the whole neutron producing sphere (Fig. 4). For this case it follows from Eqn. 3, Eqn. B-10 and integrating  $\cos\psi_0$  in Eqn. 3 over the whole range +1 to -1

$$J_0(\vec{r}, T)\Delta T = N_0 \left( \frac{2\pi KT}{m} \right)^{-3/2} \frac{v^2 \Delta v}{2R^2} \left\{ \frac{KT}{mv_0 v} \left[ e^{-\frac{m}{2KT} (v-v_0)^2} - e^{-\frac{m}{2KT} (v+v_0)^2} \right] \right\}$$

EQN 15

As in the pencil model we assume again that  $\beta = 1$ , and, after multiplying Eqn. 15 by  $\pi r^2$ , obtain

$$\pi r^2 J_0(\vec{r}, T)\Delta T = \frac{r^2}{4R^2} \frac{N_0}{\sqrt{\pi}} v^2 \Delta v \left\{ \frac{1}{v} \left[ e^{-(v-1)^2} - e^{-(v+1)^2} \right] \right\}$$

EQN 16

where  $v = \frac{v}{v_0}$ ,  $v_0 = \sqrt{\frac{2KT}{m}}$ ,  $N_0 =$  total thermal neutrons produced.

Equation 16 gives the total neutrons passing through the aperture area  $\pi r^2$  (cm<sup>2</sup>) on top of the pipe perpendicular to  $\vec{n}_0$  at distance R (cm) from the source.

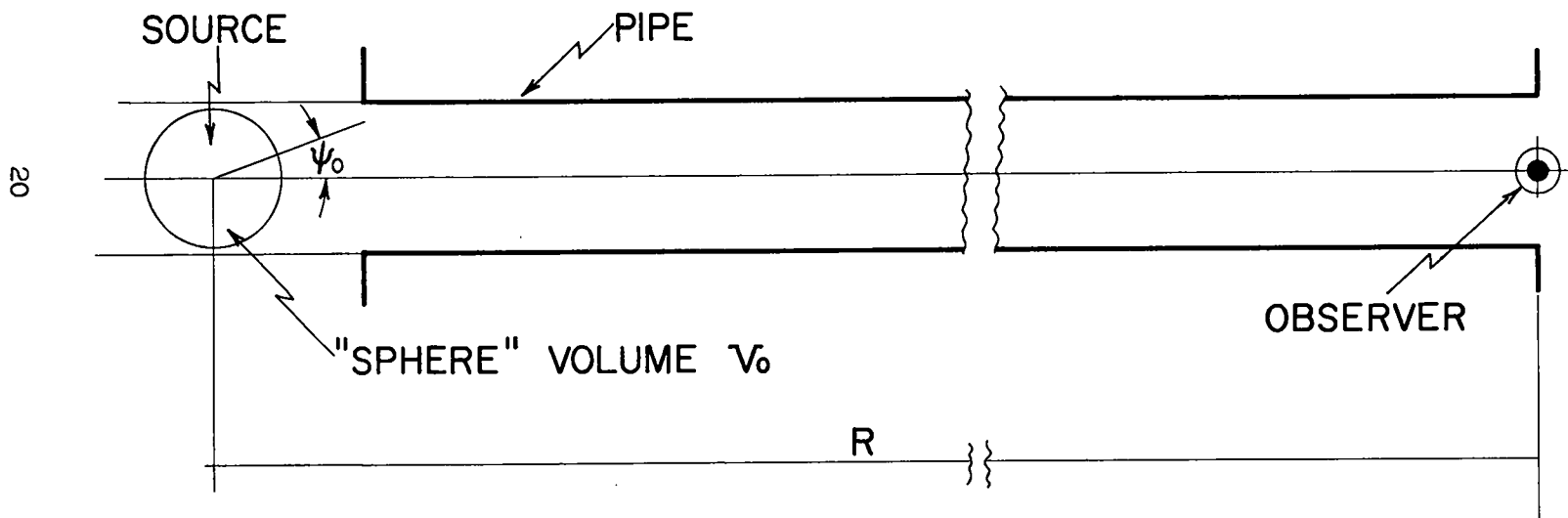


FIG. 4. "SPHERE" MODEL OF DEBRIS SPHERE AND PIPE.

For comparison, we again give below the corresponding equation for the hypothetical case of  $v_0 = 0$ .

$$\pi r^2 J_0(\vec{r}, T) \Delta T = \frac{r^2}{2R^2} \frac{N_0}{\sqrt{2\pi}} \frac{v^2 \Delta v}{\sqrt{\frac{KT}{m}} \frac{KT}{m}} e^{-\frac{m}{2KT} v^2} \quad \text{EQN 16a}$$

## V. NUMERICAL EVALUATION OF "PARROT" ESCAPE SPECTRUM

The experimental set-up (Fig. 5) has been described in the open literature.<sup>3</sup>

The numerical values for the quantities shown in Fig. 5 are listed below. These values are subsequently used to numerically evaluate Eqn. 14 "pencil" model and Eqn. 16 "sphere" model.

$N_0 = 0.06848 \times 10^{24}$	"Parrot" neutrons released in thermal equilibrium
$V_0 = 5.24 \times 10^5 \text{ cm}^3$	Bomb debris "sphere" volume at time of neutron release
$U_0 = 3.24 \times 10^4 \text{ cm}^3$	Bomb debris "pencil" volume at time of neutron release
$R = 182.18 \text{ m}$	Distance bomb debris center to fission foil detector of area $\pi r^2 = 1.037 \text{ cm}^2$ pipe radius
	$\eta = 10.16 \text{ cm}$
$Y = 1.2 \text{ KT}$	Total yield of "Parrot"
$KT = 474 \text{ ev}$	Bomb thermal temperature
$v_0 = 0.3 \text{ cm/sh}$	Material velocity

These individual quantities shown in Fig. 5 will now be discussed briefly.

---

<sup>3</sup>"Neutron Time of Flight Experiments Using Nuclear Explosions," B. C. Diven. Submitted and to be published in Oct. 1965 issue of SCIENCE.



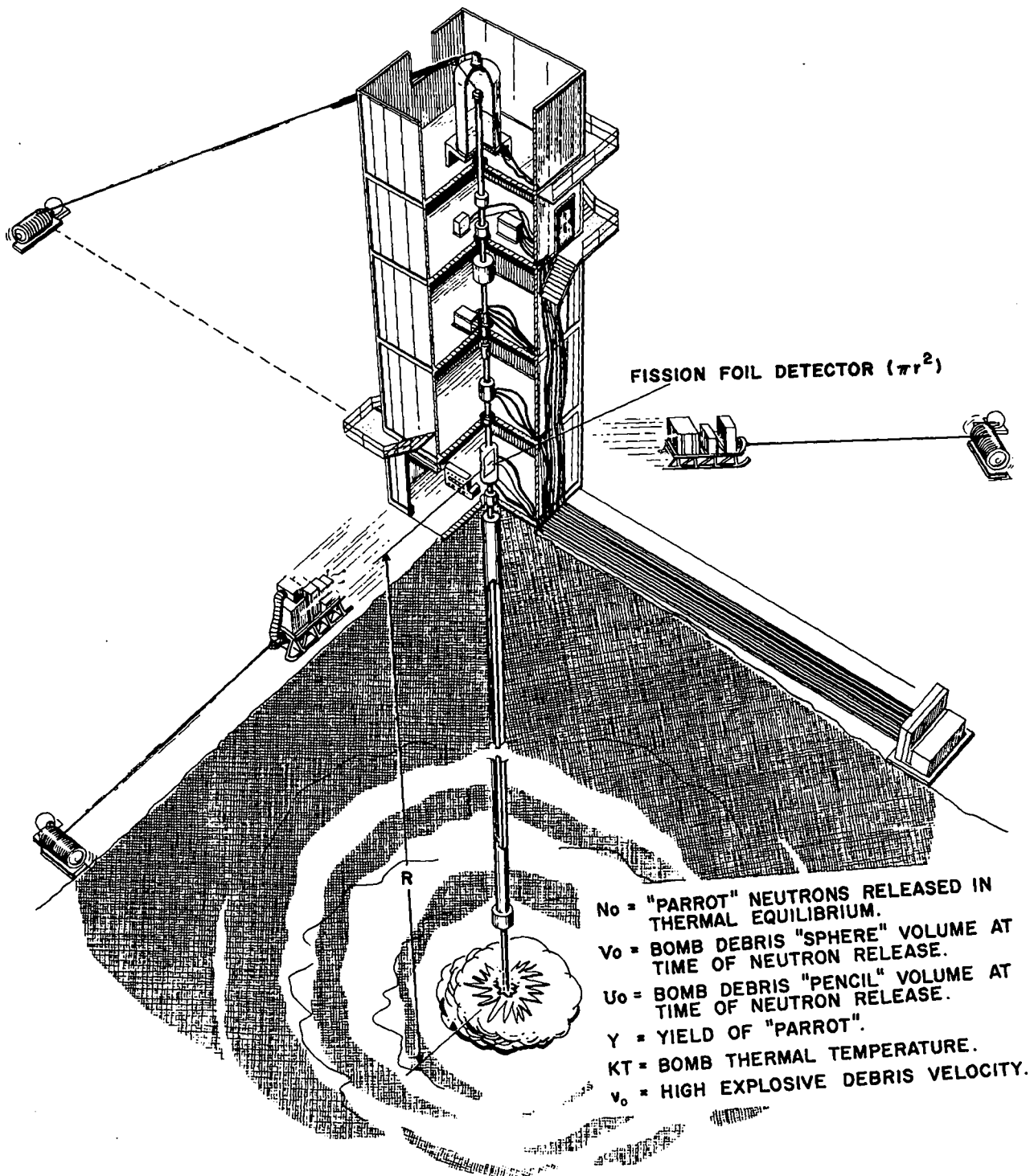


FIG. 5. UNDERGROUND NUCLEAR TEST "PARROT."

- a.  $N_0$ , Parrot neutrons released in thermal equilibrium;  $v_0$ , debris velocity and  $KT$ , Parrot bomb thermal temperature.

In a nuclear device a configuration of fissionable material is driven together by exploding the surrounding high explosive layer.

The assembled configuration will reach supercriticality and the released fission energy will cause the rapid expansion of the bomb. The debris will move radially outward, including the heterogeneous remnants of the high explosive layer. Before the high explosive moderator or reflector moves away, it is assumed that the fission neutrons born have come to a thermal equilibrium by collisions with the bomb debris.

During the expansion phase a time will be reached where the surrounding moderator (high explosive remnants) comes to such a low density that the thermal neutrons will cease to make collisions with the high explosive debris. We are therefore confronted with the problem to determine the neutron spectrum coming from a moving source, as seen in the Laboratory system. The material velocity  $v_0$  of the debris becomes the source velocity of the "bottled up" thermal neutrons.

From coupled hydrodynamics--neutronics calculations--the number of thermal neutrons  $N_0$  can be determined as well as the velocity  $v_0$  of the high explosive debris. A reasonable estimate of the HE debris velocity  $v_0$  at the time of thermal neutron release is 0.3 cm/shake. The debris temperature may now be deduced by using the fact that, behind a strong shock, internal energy per gram equals kinetic energy per gram: for the

essentially completely ionized HE components, this translates to

$v_0 \simeq \sqrt{2KT/m}$  with  $m$  still representing the mass of one neutron. We thus obtain  $KT \simeq 474$  ev.

b. Pencil and sphere volume,  $V_0$  and  $U_0$ .

The volume of the debris sphere  $U_0$ , as well as the pencil volume  $V_0$ , is determined from the same calculations mentioned previously. The sphere volume  $V_0$  is the configuration in which the mean free path for thermal neutrons in the high explosive remnants becomes so large that it will no longer act as a diffusive medium for thermal neutrons.

c. Depth of underground nuclear explosion,  $R$ .

The quantity of interest in this report is  $R = 182.18$  m and the foil area  $\pi r^2 = 1.037$  cm<sup>2</sup>. The fixed aperture area just below ground level is  $0.9698$  cm<sup>2</sup>. The fission foil is a few feet above ground level.

d. Evaluation of "pencil" and "sphere" neutron spectrum.

Equations 14 and 14a, and Eqns. 16 and 16a are evaluated for even steps in the dimensionless variable  $u = v/v_0$  (Table 1). For  $u = 1$  the neutron velocity  $v$  traveling up the pipe is equal to  $v_0$ , the debris velocity. Table 1 assumes a bomb thermal temperature of 474 ev. Columns 2 through 8 are evaluated from the following relationships

$$v = u \times v_0 = 0.3u \text{ (cm/sh)}$$

$$\Delta v = \Delta u \times v_0 = 0.3\Delta u \text{ (cm/sh)}$$

$$E(\text{Mev}) = \frac{[v(\text{cm/sh})]^2}{(13.827)^2}$$

$$\Delta E(\text{Mev}) = v(\text{cm/sh}) \Delta v(\text{cm/sh}) \frac{2}{(13.827)^2}$$

$$T(\text{sh}) = \frac{R(\text{cm})}{v(\text{cm/sh})} = \frac{1.8218 \times 10^4}{v(\text{cm/sh})}$$

$$\Delta T(\text{sh}) = \frac{R(\text{cm})\Delta v(\text{cm/sh})}{[v(\text{cm/sh})]^2} = \frac{1.8218 \times 10^4 \Delta v(\text{cm/sh})}{[v(\text{cm/sh})]^2}$$

Note that the intervals  $\Delta v$ ,  $\Delta E$  and  $\Delta T$  follow from the arbitrarily chosen interval  $\Delta v$ .

The numerical expression to evaluate  $J_0(\vec{r}, T)$  in Table 1 for all models and assumptions are listed below.

"Pencil" model;  $v_0 = 0.3 \text{ cm/sh}$ ;  $v_0 = \sqrt{\frac{2KT}{m}}$

Table 1, Column 9.  $KT = 474 \text{ ev.}$

From Eqn. 14 we get

$$\pi r^2 J_0(\vec{r}, T) \Delta T = 1.1878 \times 10^{12} v^2 \Delta v \left[ e^{-(v-1)^2} + e^{-(v+1)^2} \right] \quad \text{EQN 17}$$

"Pencil" model;  $v_0 = 0$ , Maxwellian;  $\sqrt{\frac{2KT}{m}} = 0.3 \text{ cm/sh}$

Table 1, Column 10.  $KT = 474 \text{ ev.}$

From Eqn. 14a we get

$$\pi r^2 J_0(\vec{r}, T) \Delta T = 8.7985 \times 10^{-11} v^2 \Delta v e^{-1.1111 \times 10^{-15} v^2} \quad \text{EQN 18}$$

"Sphere" model;  $v_0 = 0.3$  cm/sh;  $v_0 = \sqrt{\frac{2kT}{m}}$

Table 1, Column 11.

$kT = 474$  ev.

From Eqn. 16 we get

$$\pi r^2 J_0(\vec{r}, T) \Delta T = 9.6047 \times 10^{-12} v^2 \Delta v \left\{ \frac{1}{v} \left[ e^{-(v-1)^2} - e^{-(v+1)^2} \right] \right\} \quad \text{EQN 19}$$

-----  
 "Sphere" model;  $v_0 = 0$ , Maxwellian;  $\sqrt{\frac{2kT}{m}} = 0.3$  cm/sh

Table 1, Column 12.

$kT = 474$  ev.

From Eqn. 16a we get

$$\pi r^2 J_0(\vec{r}, T) \Delta T = 1.4263 \times 10^{-9} v^2 \Delta v e^{-1.1111 \times 10^{-15} v^2} \quad \text{EQN 20}$$

For our case  $\pi r^2 = 1.037$  cm<sup>2</sup> and  $\Delta T$  is taken from Table 1.

The last four columns of Table 1, as well as the experimental data, are plotted in Fig. 6.

The experimental data agree reasonably well with the calculated pencil model values. The neutron flux is "contaminated" with "reflected" neutrons which are not included in our calculations. The first peak at 18 ev is probably due to reflected neutrons from the bottom of the hole which picked up some energy from the "pre-heated" lining of the cavity. At higher energies above 3 kev we get the neutrons which have been slowed down from higher energies. This energy range is not included in this discussion, as we limited ourselves to the thermal part.

v	$\Delta v$	v (cm/sh)	$\Delta v$ (cm/sh)	E	$\Delta E$ (ev)	T (msec)	$\Delta T$ ( $\mu$ sec)	$J_0(\vec{r}, T)$			
								Neutrons/cm <sup>2</sup> sec; KT = 474 ev; R = 182.18 m			
								"Pencil"		"Sphere"	
$v_0 = 0.3$ cm/sh	Maxwell $v_0 = 0$	$v_0 = 0.3$ cm/sh	Maxwell $v_0 = 0$								
0.1	0.05	0.03	0.015	0.47 ev	4.71	6.073	3030	$1.405 \times 10^{11}$	$3.742 \times 10^{11}$	$2.242 \times 10^{12}$	$6.067 \times 10^{12}$
0.2	0.05	0.06	0.015	18.8 ev	9.41	3.036	759.1	$2.307 \times 10^{12}$	$5.799 \times 10^{12}$	$3.544 \times 10^{13}$	$9.400 \times 10^{13}$
0.3	0.05	0.09	0.015	42.4 ev	14.12	2.024	337.4	$1.218 \times 10^{13}$	$2.792 \times 10^{13}$	$1.763 \times 10^{14}$	$4.526 \times 10^{14}$
0.4	0.05	0.12	0.015	75.3 ev	18.83	1.518	189.8	$4.048 \times 10^{13}$	$8.228 \times 10^{13}$	$5.432 \times 10^{14}$	$1.334 \times 10^{15}$
0.5	0.05	0.15	0.015	117.7 ev	23.54	1.215	121.5	$1.042 \times 10^{14}$	$1.836 \times 10^{14}$	$1.283 \times 10^{15}$	$2.976 \times 10^{15}$
0.6	0.05	0.18	0.015	169.5 ev	28.24	1.012	84.3	$2.273 \times 10^{14}$	$3.413 \times 10^{14}$	$2.554 \times 10^{15}$	$5.533 \times 10^{15}$
0.7	0.05	0.21	0.015	230.6 ev	32.95	0.868	62.0	$4.389 \times 10^{14}$	$5.546 \times 10^{14}$	$4.487 \times 10^{15}$	$8.990 \times 10^{15}$
0.8	0.05	0.24	0.015	301.2 ev	37.66	0.759	47.4	$7.732 \times 10^{14}$	$8.155 \times 10^{14}$	$7.203 \times 10^{15}$	$1.322 \times 10^{16}$
0.9	0.05	0.27	0.015	381.3 ev	42.36	0.675	37.5	$1.258 \times 10^{15}$	$1.101 \times 10^{15}$	$1.070 \times 10^{16}$	$1.785 \times 10^{16}$
1.0	0.05	0.30	0.015	470.7 ev	47.07	0.607	30.4	$1.918 \times 10^{15}$	$1.386 \times 10^{15}$	$1.495 \times 10^{16}$	$2.247 \times 10^{16}$
1.2	0.10	0.36	0.030	678.0 ev	113	0.506	42.4	$3.787 \times 10^{15}$	$1.852 \times 10^{15}$	$2.509 \times 10^{16}$	$3.002 \times 10^{16}$
1.4	0.10	0.42	0.030	923.0 ev	132	0.434	31.0	$6.194 \times 10^{15}$	$2.041 \times 10^{15}$	$3.552 \times 10^{16}$	$3.309 \times 10^{16}$
1.6	0.10	0.48	0.030	1.21 kev	151	0.380	23.7	$8.646 \times 10^{15}$	$1.913 \times 10^{15}$	$4.354 \times 10^{16}$	$3.101 \times 10^{16}$
1.8	0.10	0.54	0.030	1.53 kev	170	0.337	18.7	$1.047 \times 10^{16}$	$1.554 \times 10^{15}$	$4.697 \times 10^{16}$	$2.519 \times 10^{16}$
2.0	0.10	0.60	0.030	1.88 kev	188	0.304	15.2	$1.109 \times 10^{16}$	$1.104 \times 10^{15}$	$4.482 \times 10^{16}$	$1.790 \times 10^{16}$
2.2	0.10	0.66	0.030	2.28 kev	207	0.276	12.5	$1.051 \times 10^{16}$	$7.015 \times 10^{14}$	$3.861 \times 10^{16}$	$1.137 \times 10^{16}$
2.4	0.10	0.72	0.030	2.71 kev	226	0.253	10.5	$8.854 \times 10^{15}$	$3.959 \times 10^{14}$	$2.983 \times 10^{16}$	$6.418 \times 10^{15}$
2.6	0.10	0.78	0.030	3.18 kev	245	0.233	8.98	$6.665 \times 10^{15}$	$1.999 \times 10^{14}$	$2.072 \times 10^{16}$	$3.240 \times 10^{15}$
2.8	0.10	0.84	0.030	3.69 kev	264	0.217	7.75	$4.538 \times 10^{15}$	$9.132 \times 10^{13}$	$1.311 \times 10^{16}$	$1.480 \times 10^{15}$
3.0	0.10	0.90	0.030	4.24 kev	282	0.203	6.75	$2.799 \times 10^{15}$	$3.757 \times 10^{13}$	$7.541 \times 10^{15}$	$6.090 \times 10^{14}$
3.2	0.10	0.96	0.030	4.82 kev	301	0.190	5.93	$1.564 \times 10^{15}$	$1.424 \times 10^{13}$	$3.953 \times 10^{15}$	$2.308 \times 10^{14}$
3.4	0.10	1.02	0.030	5.44 kev	320	0.179	5.26	$7.932 \times 10^{14}$	$5.033 \times 10^{12}$	$1.887 \times 10^{15}$	$8.159 \times 10^{13}$

TABLE 1

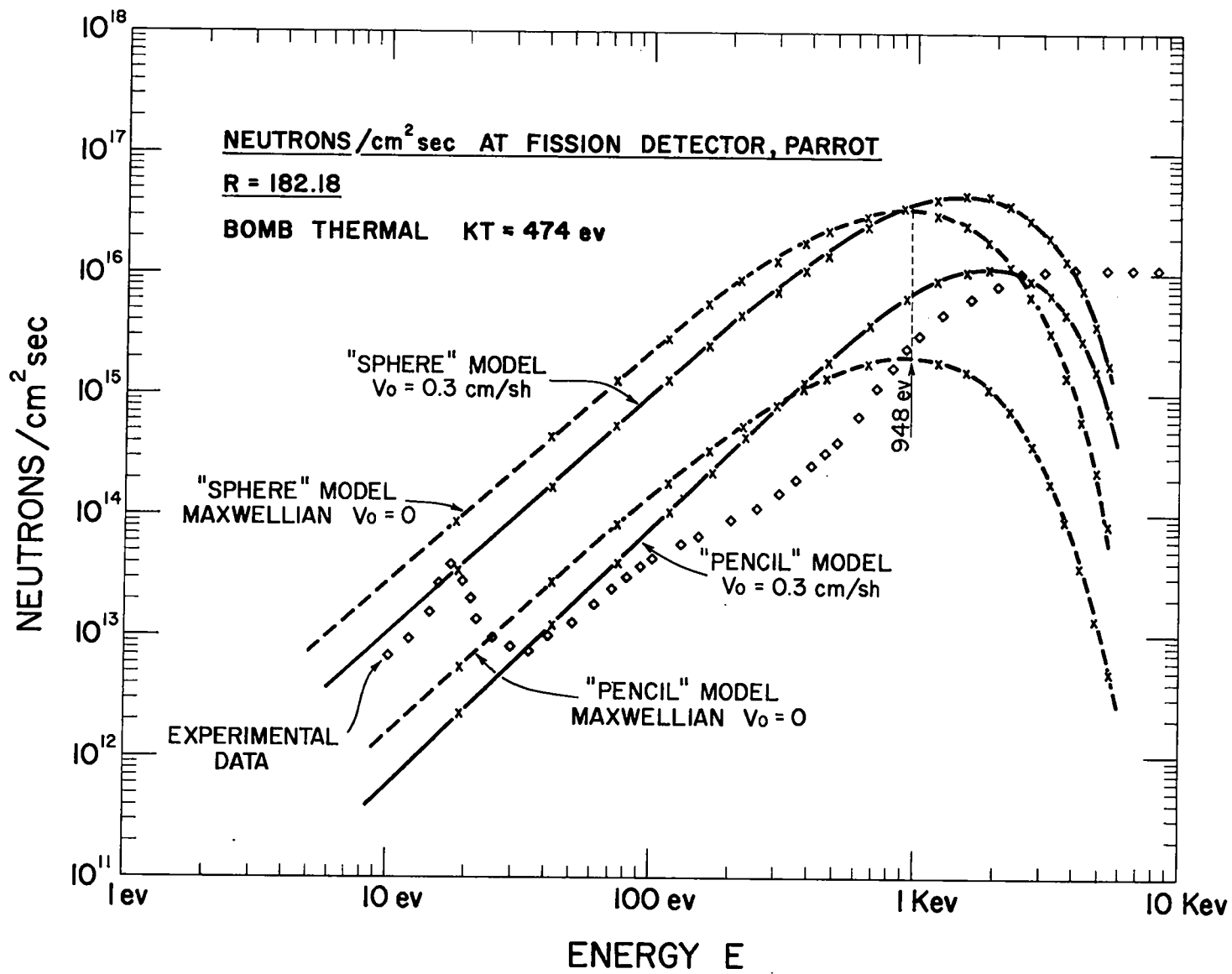


FIG. 6. THERMAL NEUTRON SPECTRA. BOMB THERMAL KT = 474 ev.

## VI. EFFECT OF FINITE BOMB DEBRIS SPHERE ON MEASUREMENT

In our derivation of  $\pi r^2 J_0(\vec{r}, T) \Delta T$  for both the "pencil" and "sphere" model, Eqns. 14, 14a, 16, and 16a, we assume that the neutrons are released from a point source. Experimentally we count and determine the energy of the arriving neutrons solely by their arrival time.

Neutrons of energy  $E$  born either on the back or front side of the debris sphere with  $\Delta R = 1$  meter (Fig. 7) will therefore arrive at different times at the fission foil detector. This difference in time of flight will be interpreted wrongly as energy differences in the point model. We will discuss the expected experimental results for a neutron energy of 8.8 ev and assuming the debris dimensions shown in Fig. 7. This particular energy is chosen since  $U^{235}$  has a strong resonance at this energy.

### Point Source, Case A.

We assume that the fission foil detector has a large and narrow resonance at  $E = 8.8$  ev. All neutrons of energy  $E = 8.8$  ev released from the point source (Fig. 7) will arrive at the fission foil detector at  $T = 4.4416 \times 10^{-3}$  sec. Since this burst of neutrons has an energy of 8.8 ev, we will detect the neutrons properly by the  $U^{235}$  resonance at 8.8 ev in the fission foil.



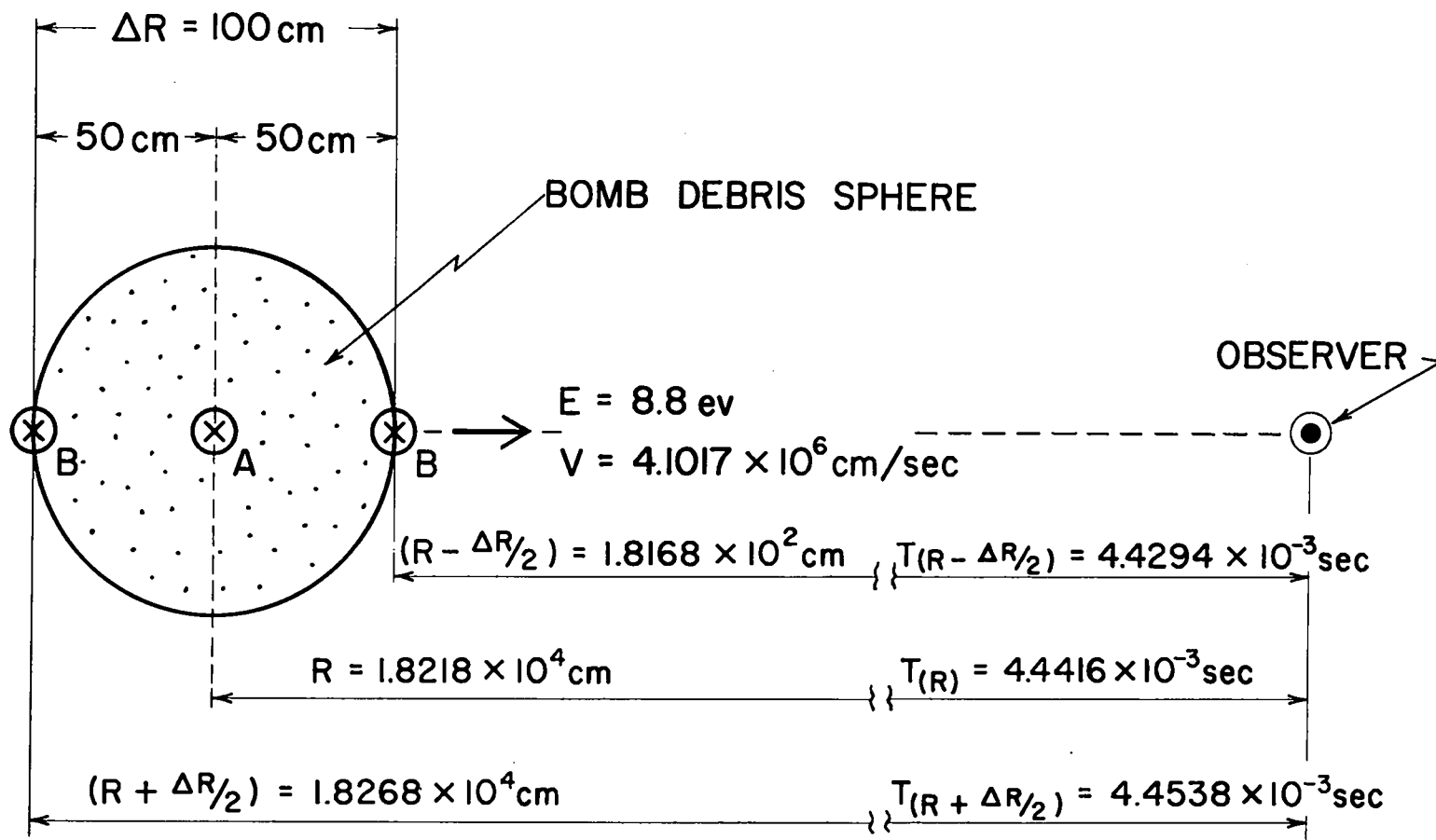


FIG. 7. MODEL A AND B FOR NEUTRON SOURCE IN DEBRIS SPHERE.

This correlation of the emitted neutron energy, the arrival time and the known resonance in the fission foil represents an effective checking mechanism on the neutron energy which arrives at the fission foil. Since the neutron arrival time is the "sole" quantity which determines the energy, we might easily be misled by neutrons of different energy which have been "bouncing" around in a non-direct pattern and just happen to arrive at the same time as the "direct" neutrons. This uncertainty can be discarded if one exposes a fission foil with known resonance structure. If one picks up these resonances, demonstrated by increased counts in the time sweep, we know that these are indeed neutrons corresponding to energies of the individual resonances.

Source at Front and Back, Case B.

Case A made the assumption that all neutrons are released from an ideal point source. We now assume that half the neutrons ( $E = 8.8$  ev) of the point source are released from the front and the other half from the back of the bomb (Fig. 7). Since we determine neutron energy by arrival time, we will interpret the differences in arrival time due to different source locations as differences in the neutron energy. We ask what this apparent energy would be for both "front" and "back" neutrons if the neutrons have been released at the source with  $E = 8.8$  ev. We also assume again that the fission foil has a resonance at this energy. Neutrons with  $E = 8.8$  ev from the front arrive at  $4.4294 \times 10^{-3}$  sec and from the back at  $4.4538 \times 10^{-3}$  sec. The apparent energy difference is

$$\frac{\Delta E}{E} = \frac{2\Delta R}{R} = \frac{2 \times 8.8 \times 100}{1.8218 \times 10^4} = 9.6608 \times 10^{-2} \quad \text{EQN 21}$$

$$\Delta E_{(E=8.8 \text{ ev})} = 0.0966 \text{ ev.}$$

Figure 8 shows the recorded counts for Case A and B.

If the separation of the two peaks (Case B) is larger than 0.08 ev, we can deduce that the source must be outside the debris sphere of  $\Delta R = 100$  cm. This can be the case if fast neutrons escape the debris, and are subsequently reflected from the bottom of the hole which contained the device. These reflected neutrons can be moderated in the soil and will find their way back up the pipe. Cold neutrons can also pick up energy from the shock heated lining of the hole. Since the neutron energy is determined solely from arrival time, it will not tell us their past energy history. It is, therefore, quite difficult to accurately say much about neutrons which did not arrive at the detector in a straight time of flight fashion from the bomb debris.

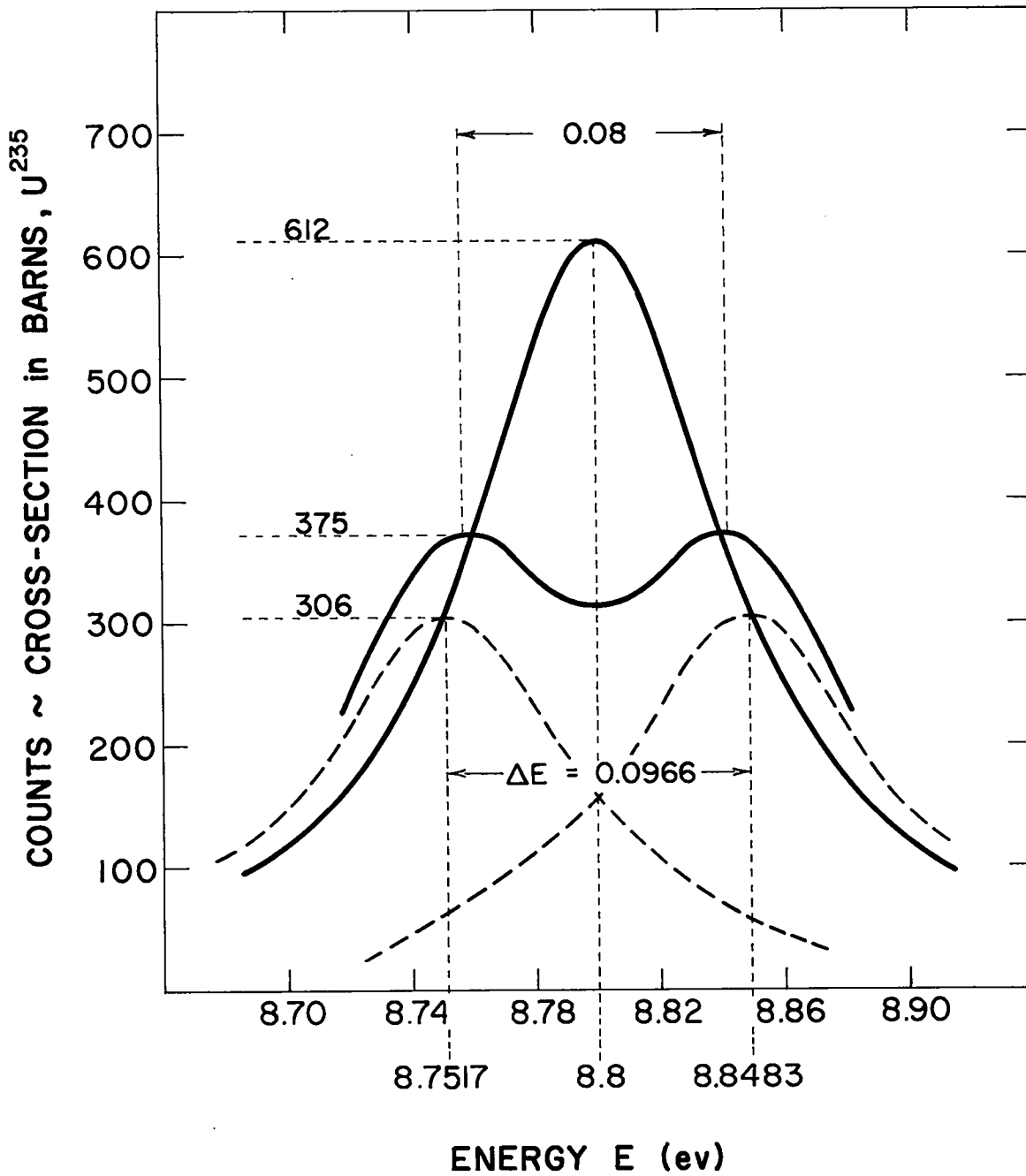


FIG. 8. COUNTS AT DETECTOR FOR DEBRIS SPHERE MODEL A AND B.

## APPENDIX A

The distribution in flight time of neutrons reaching a detector remote from a pulsed source.

Theory.

We assume a localized neutron source  $S(\vec{r}, E, \vec{\Omega}, t)$  according to Fig. A-1.

Boltzmann Equation.

$$\frac{1}{v} \frac{\partial \varphi(\vec{r}, E, \vec{\Omega}, t)}{\partial t} + \vec{\Omega}_0 \cdot \nabla \varphi(\vec{r}, E, \vec{\Omega}, t) = S(\vec{r}, E, \vec{\Omega}, t) \quad \text{EQN A-1}$$

Here the usual scattering term is missing since we assume vacuum between the source and the observer.

Integral Form.

$$\varphi(\vec{r}, E, \vec{\Omega}, t) = \int_{\mathcal{L}} S(\vec{r} - \vec{\Omega}l, E, \vec{\Omega}, t - \frac{l}{v}) dl \quad \text{EQN A-2}$$

Here neutrons which leave the source at  $t - l/v$  with constant velocity  $v$  arrive at the observer at time  $t$ . In the integral form the second term in Eqn. A-1 becomes zero due to the assumed  $\delta$ -function source pulse width.

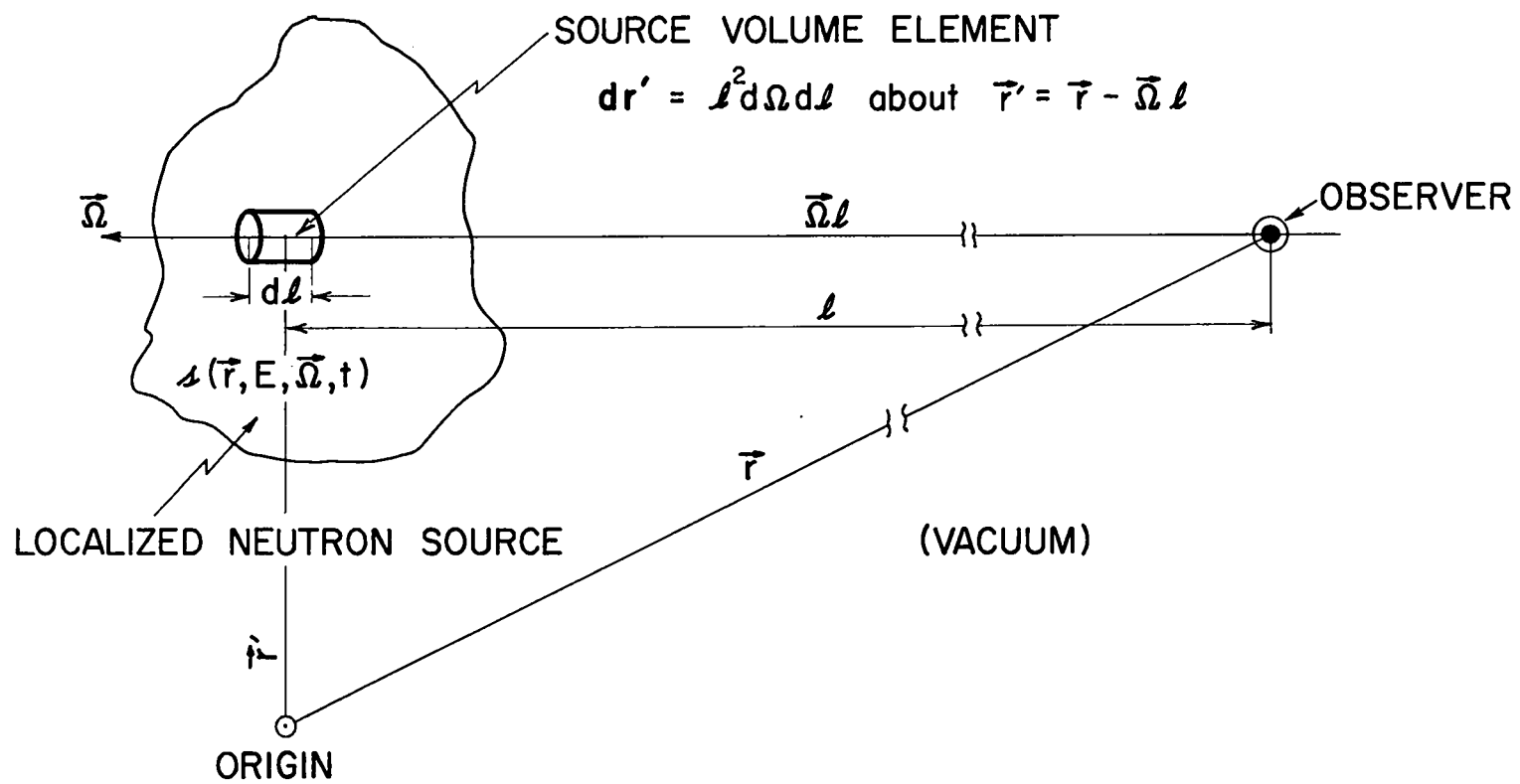


FIG. A-1. SOURCE--OBSERVER CONFIGURATION.

Total flux at point of observer

$$\begin{aligned} \Phi(\vec{r}, E, t) &= \int_{\vec{\Omega}} \varphi(\vec{r}, E, \vec{\Omega}, t) d\Omega = \int_{\ell} \int_{\vec{\Omega}} \mathfrak{S}(\vec{r}-\vec{\Omega}\ell, E, \vec{\Omega}, t-\frac{\ell}{v}) d\ell d\Omega & \text{EQN A-3} \\ &= \int_{\text{source}} \mathfrak{S}\left(\vec{r}', E, \frac{\vec{r}-\vec{r}'}{\ell}, t-\frac{\ell}{v}\right) \frac{dr'}{\ell^2} \end{aligned}$$

Total current at point of observer

$$\begin{aligned} \vec{J}(\vec{r}, E, t) &= \int_{\vec{\Omega}} \varphi(\vec{r}, E, \vec{\Omega}, t) \vec{\Omega} d\Omega \\ &= \int_{\ell} \int_{\vec{\Omega}} \mathfrak{S}(\vec{r}-\vec{\Omega}\ell, E, \vec{\Omega}, t-\frac{\ell}{v}) \vec{\Omega} \ell d\ell d\Omega \\ &= \int_{\text{source}} \left(\frac{\vec{r}-\vec{r}'}{\ell}\right) \mathfrak{S}\left(\vec{r}', E, \frac{\vec{r}-\vec{r}'}{\ell}, t-\frac{\ell}{v}\right) \frac{dr'}{\ell^2} & \text{EQN A-4} \end{aligned}$$

Delta Function Source.

$$\mathfrak{S}(\vec{r}', E, \vec{\Omega}, t) = \mathfrak{S}_0(\vec{r}', E, \vec{\Omega}) \delta(t) \quad \text{EQN A-5}$$

We now integrate the Boltzmann equation, Eqn. A-1, from  $0^- \leq t \leq 0^+$  and obtain the initial neutron population created by the  $\delta$ -function source at  $\vec{r}'$ .

$$\frac{\varphi(\vec{r}', E, \vec{\Omega}, 0^+)}{v} = n(\vec{r}', E, \vec{\Omega}, 0^+) = s_o(\vec{r}', E, \vec{\Omega}) \quad \text{EQN A-6}$$

From Eqn. A-6 and Eqn. A-3 we set for the total flux at the point of observer  $\vec{r}$ .

$$\phi(\vec{r}, E, t) = \int_{\text{source}} n(\vec{r}', E, \frac{\vec{r}-\vec{r}'}{\ell}, 0^+) \delta\left(t-\frac{\ell}{v}\right) \frac{dr'}{\ell^2} \quad \text{EQN A-7}$$

The total flux  $\phi$  at the observer is due to the initial neutron density  $n$  at time  $0^+$  on the spherical surface  $(\vec{r}' - \vec{r}) = \ell$ .

For a localized source and distant field point  $\vec{r}$ , say the distance  $R$  from the source center, what is the total current passing through a unit area at  $\vec{r}$  in the time interval  $\Delta T$  at  $T$ ? The above statement implies that the source dimension  $\Delta R$  is small compared with  $R$ , the distance between the source and the observer.  $\Delta T$  is, therefore, large compared to the neutron transit time across the source (assuming constant velocity) but still small (increment) compared to the flight time from the source to the observer.

$$\begin{aligned} \vec{J}_o(\vec{r}, T) \Delta T &= \int_{T-\frac{\Delta T}{2}}^{T+\frac{\Delta T}{2}} dt \int_0^\infty dE \vec{J}(\vec{r}, E, t) \\ &= \int_{T-\frac{\Delta T}{2}}^{T+\frac{\Delta T}{2}} dt \int_0^\infty dE \int_{\text{source}} \left(\frac{r-r'}{\ell}\right) n(\vec{r}', E, \frac{\vec{r}-\vec{r}'}{\ell}, 0^+) \delta\left(t-\frac{\ell}{v}\right) \frac{dr'}{\ell^2} \end{aligned} \quad \text{EQN A-8}$$



If one integrates Eqn. A-8 over dt first, we get

$$\vec{J}_0(\vec{R}, T) \Delta T = \int_0^{\infty} dE \int_{\text{source}} \left( \frac{\vec{R}-\vec{r}'}{l} \right) n(\vec{r}', E, \frac{\vec{R}-\vec{r}'}{l}, 0^+) \frac{dr'}{l^2} \quad \text{EQN A-9}$$

where the range of E or v and  $l(r')$  or R is restricted by

$$T - \frac{\Delta T}{2} \leq \frac{l(\vec{r}')}{v} \leq T + \frac{\Delta T}{2} \quad \text{EQN A-10}$$

Equation A-10 expresses the time of flight concept; that is, the energy of neutrons arriving at the observer is solely determined by the neutron arrival time T.

The neutron energy or velocity which is deduced from the flight time T is

$$v_{\text{max}} = \frac{R + \Delta R/2}{T - \Delta T/2} \approx \frac{R}{T - \Delta T/2}$$

$$v_{\text{min}} = \frac{R - \Delta R/2}{T + \Delta T/2} \approx \frac{R}{T + \Delta T/2}$$

or 
$$\Delta v = \frac{R}{T^2} \Delta T \quad \text{EQN A-11}$$

To better see the meaning of this approximation, we sketch Fig. A-2 on the  $l, v$  plane, that region containing  $t - l/v = 0$  for  $T - \frac{\Delta T}{2} \leq t \leq T + \frac{\Delta T}{2}$  and  $R - \frac{\Delta R}{2} \leq l \leq R + \frac{\Delta R}{2}$ .

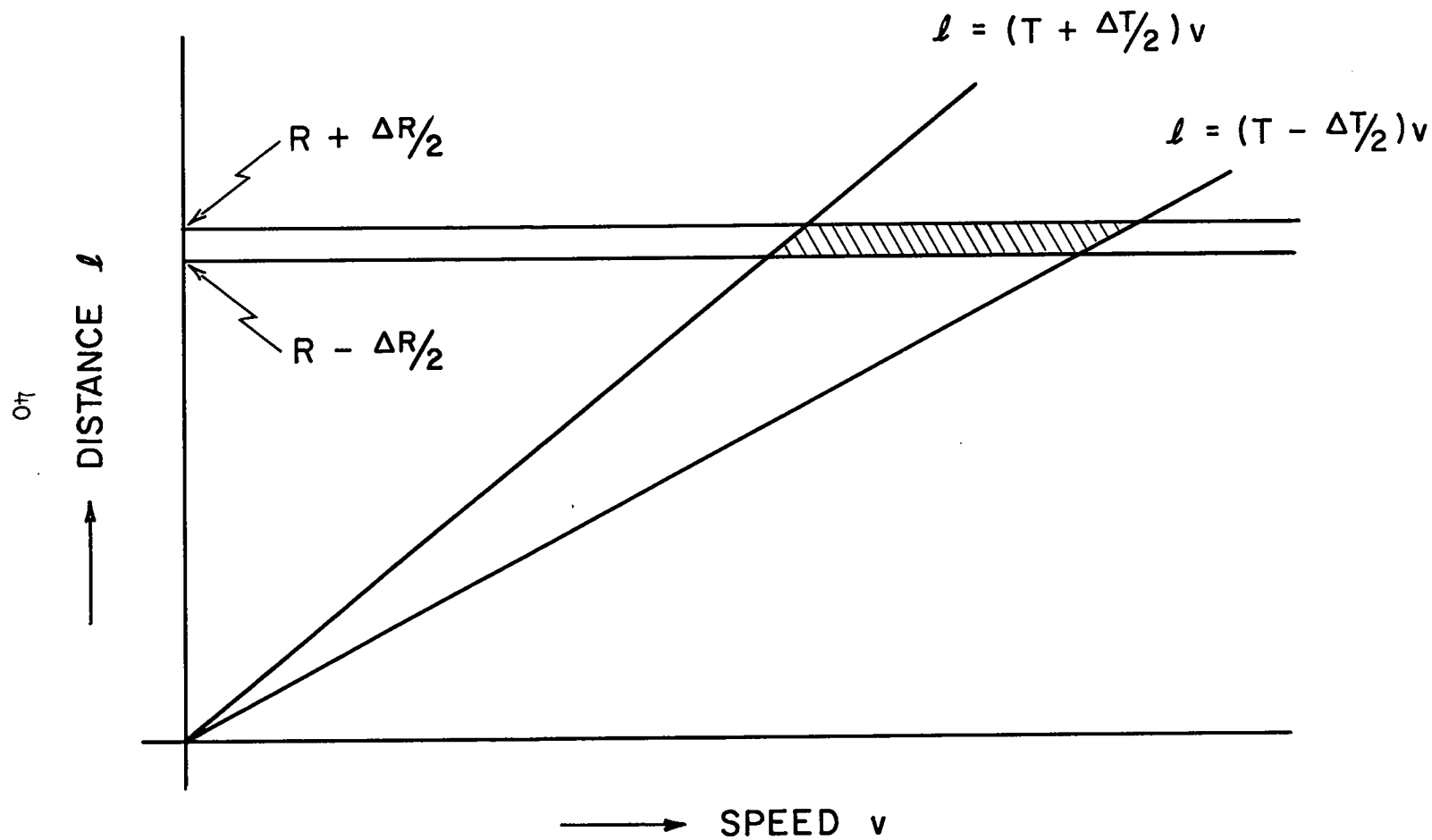


FIG. A-2. FINITE SOURCE  $\Delta R$  AND TIME OF FLIGHT.

The hashed area element in Fig. A-2 indicates the loci of  $\ell, v$  points which permit neutrons to reach the observer at  $t = T$  in  $\pm \Delta T/2$ . Our above assertion that  $\Delta T$  be large compared to the transit time of a neutron across the source (i.e.  $\Delta T \gg \Delta R/v$ ) implies that the change in  $v$  along the  $\ell = (T \pm \Delta T/2)v$  borders of this area element is small compared to the change  $\Delta v \approx v_{\max} - v_{\min}$ , along the  $\ell = R \pm \Delta R/2$  borders. The approximation, that  $v$  and  $T$  (or  $E$  and  $T$ ) are functionally related, breaks down for the time resolution  $\Delta T = \Delta R/v$ , and this corresponds to a velocity (speed) or energy resolution

$$\frac{\Delta v}{v} \approx \frac{\Delta R}{R} \approx \frac{\Delta E}{2E} \quad \text{EQN A-12}$$

For the case of interest in this report  $\frac{\Delta R}{R} \approx 0.005$ . For  $E = 10$  ev we get therefore for  $\Delta E = 0.108$  ev. For the above numerical example the uncertainty in the source position produces an uncertainty in the energy of 0.1 ev.

In Eqn. A-9 we change the variable  $E$  to  $v$ .

$$\vec{J}_O(\vec{r}, T) \Delta T = \int_{\text{source}} d\vec{r}' \left( \frac{\vec{r} - \vec{r}'}{\ell} \right) n \vec{r}', v, \frac{\vec{r} - \vec{r}'}{\ell}, 0^+ \frac{\Delta v}{\ell^2} \quad \text{EQN A-13}$$

Since

$$\left( \frac{\vec{r} - \vec{r}'}{\ell} \right) \approx \frac{(\vec{r} - \vec{r}')_{ct.}}{R} = \vec{\Omega}_O$$

and

$$\vec{J}_0 = J_0 \vec{\Omega}_0$$

$$J_0(\vec{r}, T) \Delta T = \int_{\text{source}} d\vec{r}' n(\vec{r}', v, \vec{\Omega}_0, 0^+) \frac{\Delta v}{R^2} \quad \text{EQN A-14}$$

where

$$v = \frac{R}{T} = \sqrt{\frac{2E}{m}}$$

$$\Delta v = R \frac{\Delta T}{T^2}; \quad \Delta E = \frac{mR}{T} \Delta v$$

Equation A-14 gives the number of neutrons passing through the unit area perpendicular to  $\vec{\Omega}_0$  at  $\vec{r}$  in the time interval  $\Delta T$  about  $T$  in terms of that portion of the initial neutron population at  $\vec{r}'$  with energies specified by  $\Delta v$  about  $v$ . The conversion from the time distribution function,  $J_0(\vec{r}, T)$ , to an energy distribution function, say  $J_0(\vec{r}, E)$  neutrons per  $\text{cm}^2$  per unit energy interval, or a velocity (speed) distribution function, say  $J_0(\vec{r}, v)$ , is readily accomplished through the obvious relations

$$J_0(\vec{r}, T) \Delta T = J_0(\vec{r}, E) \Delta E = J_0(\vec{r}, v) \Delta v \quad \text{EQN A-15}$$

## APPENDIX B

### Total source strength.

We want to determine factor  $c$  in Eqn. 1. The total neutrons produced are

$$N_0 = \int_{\text{source}} d\mathbf{r}' \int_v dv \int_{\vec{\Omega}} d\Omega \int_t dt \mathcal{S}(\mathbf{r}', v, \vec{\Omega}, t) \quad \text{EQN B-1}$$

The initial neutrons are produced instantaneously by a  $\delta$ -function source

$$N_0 = \int_{\text{source}} d\mathbf{r}' \int_v dv \int_{\vec{\Omega}} d\Omega n(\vec{\mathbf{r}}', v, \vec{\Omega}, 0^+) \quad \text{EQN B-2}$$

The initial neutron population  $n(\vec{\mathbf{r}}', v, \vec{\Omega}, 0^+)$  created by the  $\delta$ -function source is as in Eqn. 2.

$$n(\vec{\mathbf{r}}', v, \vec{\Omega}, 0^+) = ce^{-\frac{m}{2KT} (v^2 + v_0^2 - 2vv_0 \cos\psi_0)} \times v^2 \quad \text{EQN B-3}$$

In Eqn. 2 we had the preferred direction  $\vec{\Omega}_0$ , but here we want to integrate over all directions  $\vec{\Omega}$ . We also make the same assumption as in Eqn. 3 that the neutrons are produced uniformly over the sphere.

Inserting Eqn. B-3 into Eqn. B-2 we get

$$N_o = \int_{\text{source}} dr' \int_v dv \int_{-1.0}^{+1.0} 2\pi d\cos\psi_o ce^{-\frac{m}{2KT}(v^2+v_o^2-2vv_o\cos\psi_o)} \times v^2 \text{ EQN B-4}$$

Here the limits of the last integral are inverted since  $d\Omega = 2\pi \sin\psi_o d\psi_o = -2\pi d\cos\psi_o$ . The last integral over the angle  $\psi_o$  we can readily integrate over its limits. We get

$$N_o = \int_{\text{source}} dr' \int_0^\infty dv \frac{2\pi cvKT}{mv_o} \left[ e^{-\frac{m}{2KT}(v-v_o)^2} - e^{-\frac{m}{2KT}(v+v_o)^2} \right] \text{ EQN B-5}$$

First we integrate Eqn. B-2 over v. We integrate the two exponential terms separately. The first term is

$$\begin{aligned} \int_0^\infty v dv e^{-\frac{m}{2KT}(v-v_o)^2} &= \int_0^\infty (v-v_o) d(v-v_o) e^{-\frac{m}{2KT}(v-v_o)^2} \\ &+ \int_0^\infty v_o d(v-v_o) e^{-\frac{m}{2KT}(v-v_o)^2} \\ &= \frac{KT}{m} \int_{x_o}^\infty dx_1 e^{-x_1^2} + v_o \sqrt{\frac{2KT}{m}} \int_{-y_o}^\infty dy_1 e^{-y_1^2} \end{aligned} \text{ EQN B-6}$$

The second term is

$$\begin{aligned}
 \int_0^{\infty} v dv e^{-\frac{m}{2KT} (v+v_0)^2} &= \int_0^{\infty} (v+v_0) d(v+v_0) e^{-\frac{m}{2KT} (v+v_0)^2} \\
 &- \int_0^{\infty} v_0 d(v+v_0) e^{-\frac{m}{2KT} (v+v_0)^2} \\
 &= \frac{KT}{m} \int_{x_0}^{\infty} dx_2 e^{-x_2^2} - v_0 \sqrt{\frac{2KT}{m}} \int_{y_0}^{\infty} dy_2 e^{-y_2^2}
 \end{aligned}
 \tag{EQN B-7}$$

The difference between Eqn. B-6 and Eqn. B-7 is

$$v_0 \sqrt{\frac{2KT}{m}} \int_{-\infty}^{+\infty} dy e^{-y^2} = v_0 \sqrt{\frac{2\pi KT}{m}}
 \tag{EQN B-8}$$

Equation B-5 now becomes

$$N_0 = \frac{2\pi cKT}{m} \sqrt{\frac{2\pi KT}{m}} \int_{\text{source}} dr'
 \tag{EQN B-9}$$

We can now determine the constant c

$$c = \frac{N_0}{V_0} \left( \frac{2\pi KT}{m} \right)^{-3/2}
 \tag{EQN B-10}$$

where  $N_0$  = Total thermal neutrons produced in sphere

$V_0$  = Source volume in  $\text{cm}^3$

$\sqrt{\frac{kT}{m}}$  = Most probable neutron velocity in Boltzmann distribution



APPENDIX C

Relationship between  $N(t)$  (neuts/cm<sup>2</sup>/sec) at fission foil and  $n(E)$  (neuts/Mev) at point of explosion.

The following relationship holds

$$N(t)dt = n(E)dE \frac{\pi r^2}{4\pi R^2} \quad \text{EQN C-1}$$

where  $\pi r^2/4\pi R^2 = 2.486 \times 10^{-10}$  geometric attenuation factor. We first determine  $dt$

$$t(\text{sec}) = \frac{R}{v} = \frac{1.8218 \times 10^4 \text{ cm}}{13.827 \sqrt{E(\text{Mev})} \times 10^8 \text{ (cm/sec)}}$$

$$= 1.317 \times 10^{-5} E(\text{Mev})^{-1/2}$$

$$dt = E^{-3/2} dE \frac{1.317 \times 10^{-5}}{2}$$

Substituting  $dt$  into Eqn. 26

$$N(t) = n(E) \frac{dE}{dt} = n(E) E^{3/2} \frac{2}{1.317 \times 10^{-5}} \times 2.486 \times 10^{-10}$$

We finally get

$$N(t) = 3.775 \times 10^{-5} E^{3/2} (\text{Mev}) n(E) \quad \text{EQN C-2}$$

Equation C-2 is the conversion formula to convert virgin escape neutrons from the bomb  $n(E)$  in neutrs/Mev to  $N(t)$ , the neutron flux in neutrons/cm<sup>2</sup> sec at the fission foil of area  $\pi r^2 = 1.037 \text{ cm}^2$  at  $R = 182.18 \text{ m}$ . The quantity  $n(E)$  in neutrs/Mev is a convenient quantity in bomb diagnostics, since the integral over energy of  $n(E)$  represents the total number of neutrons leaking from the device, which can be directly related to such quantities as the yield of Parrot and fission neutrons born.